Natural Hazards
and Earth System
Sciences

Open Access

EGU

Discussions

# High-spatial resolution probability maps of drought duration and magnitude across Spain

Fernando Domínguez-Castro[1], Sergio M. Vicente-Serrano[1], Miquel Tomás-Burguera[2], Marina Peña-Gallardo[1], Santiago Beguería[2], Ahmed El Kenawy[1,3], Yolanda Luna[4], Ana Morata[4]

[1]Instituto Pirenaico de Ecología, Spanish National Research Council (IPE-CSIC), Zaragoza, 50059, Spain
[2]Estación Experimental de Aula Dei, Spanish National Research Council (EEAD-CSIC), Zaragoza, 50059, Spain
[3]Department of Geography, Mansoura University, Mansoura, 35516, Egypt
[4]Agencia Estatal de Meteorología (AEMET), Madrid, 28071, Spain

*Correspondence to*: Fernando Domínguez-Castro (f.dominguez.castro@gmail.com)

**Abstract.** We mapped—for the first time—the probability of occurrence of drought over Spain, with the overriding aim of improving current drought assessment, management and mitigation measures and strategies across the region. We employed two well-established drought indices: the Standardized Precipitation Index (SPI) and the Standardized Precipitation Evapotranspiration Index (SPEI). Drought characteristics (i.e. duration and severity) were characterised at 1-, 3-, 6- and 12-month, implying that drought event is attained only when the index values are lower than zero. We applied the extreme value theory to map drought hazard probability. Following this procedure, we tested different thresholds to generate the peak-over-threshold drought severity and magnitude series, besides evaluating different three-parametric distributions and thresholds to fit these series. Our results demonstrate that the Generalized Pareto distribution performs well in estimating the frequencies of drought magnitude and duration, with good agreement between the observed and modelled data when using upper percentiles to generate the peak-over-threshold series. Spatially, our estimations suggest a higher probability of extreme drought events in southern and central areas of Spain, compared to northern and eastern regions. Nevertheless, there are strong differences in drought probability estimations between drought indices (i.e. SPI and SPEI), as well as among drought timescales.

## 1 Introduction

Drought is one of the main hydro-climatic hazards in Spain, with adverse impacts on natural and human environments (Pérez and Barreiro-Hurlé, 2009; UNEP, 2006). Numerous studies have analysed drought characteristics in Spain, suggesting a strong variability over both space and time (Domínguez-Castro et al., 2018; González-Hidalgo et al., 2018). In Spain, drought management measures are usually based on insurances and government subsidies to diminish their impacts, particularly those related to agricultural sector (Fernández, 2006). In addition, there are different monitoring systems for hydrological drought conditions (Maia and Vicente-Serrano, 2017), besides large legislation practices to improve adaptation strategies and practices to drought events (Garrick et al., 2017).

Nevertheless, although current measures are quite useful to diminish drought risk in Spain, other improved approaches are still needed to reduce drought risk at the country level, including real time drought monitoring (e.g. Svoboda et al., 2002) and forecasting (e.g. Mishra et al., 2009; Mishra and Singh, 2011). In the same context, developing drought probabilities maps can be a promising tool to characterise drought risk at a more-detailed spatial scale. The utility of probabilistic

5    approaches to enhance drought monitoring and adaptation has been evidenced in many regions worldwide (e.g. Engeland et al., 2005; Hussain et al., 2018; She et al., 2014; Tosunoglu and Can, 2016; Zamani et al., 2015). According to this approach, it is possible to determine the probability of drought episodes of certain severity, allowing for establishing better sectorial management strategies. With the availability of dense spatial climatic data, it is possible to map drought probabilities at fine spatial scale, which can be useful for different socioeconomic sectors as well as management of natural ecosystems.

10   In Spain, several works have developed drought-related probability maps for Spain (e.g. Lana et al., 2006; Martin-Vide and Gomez, 1999; Pérez-Sánchez and Senent-Aparicio, 2018), but with particular emphasis on the use of dry spells obtained from daily precipitation records. Unfortunately, these studies did not account for the different drought hazard probability, given that the frequency and duration of dry spells are closely driven by the climatology of the studied area. As such, the probability of occurrence of dry spells is higher in arid regions than in humid regions. In this context, it can thus be expected

15   that a simple map of climate aridity in Spain shows similar spatial patterns to those of dry spell probability. Herein, it should be stressed that drought must be distinguished from aridity. This is simply because, irrespective of the climatology, drought can occur in any world region, when there is a temporal negative anomaly with respect to the long-term average wet conditions (Wilhite and Pulwarty, 2017). Accordingly, drought probability cannot necessarily be related to the spatial patterns of climate aridity, but it is rather associated with the intrinsic characteristics of drought events recorded in each

20   region. This highlights the importance of normalizing data of climatic variables for common periods to make drought conditions (e.g. duration, intensity, severity) comparable among regions with different climatic conditions.  In this regard, drought indices can be seen as useful tools for characterising drought conditions across regions with different climatic conditions (Redmond, 2002). Moreover, drought indices allow for identifying drought episodes that can be defined according to their duration and magnitude (Dracup et al., 1980), which are also independent of the average climatic

25   conditions. Taken together, it is possible to employ drought indices to create detailed maps of the probability of occurrence of drought severity, which characterises these drought episodes from a stochastic point of view. Some studies have developed this idea in different regions, for example, in their assessment of drought characteristics in Serbia, Tošić and Unkašević (2014) analysed probability of occurrence of drought using the SPI between 1949 and 2011, concluding that  the Generalized Pareto (GP) distribution fits well with the series at 1- and 12- month timescales. Similarly, Yusof et al. (2013)

30   analysed the probability of drought duration and magnitude using the SPI and rainfall data from 30 rain gauges distributed across the peninsular Malaysia. Zin et al. (2013) also analysed the return period for drought severity over the peninsular Malaysia by means of the SPI. A quick inspection of these studies reveals that they employed an individual drought index (SPI in most cases), with few attempts to explore the possible differences in drought hazard probability, as a function of different drought indices (e.g. Yan et al., 2018) or different drought timescales (Moradi et al., 2011; Tošić and Unkašević,

2014). Due to the varying response of the different hydrological sub-systems, socioeconomic sectors and natural ecosystems to drought timescales, it is well-recognized that drought timescales should be taken into account when determining drought impacts (McKee et al., 1993; Vicente-Serrano, 2013). Moreover, drought patterns could differ spatially as a function of timescale (Vicente-Serrano, 2006), and correspondingly drought hazard probability can vary spatially in response to drought

5   time scale. As such, to meet the specific needs of the different socioeconomic sectors and natural systems, it is important to assess drought hazard probability at different drought timescales. Unfortunately, this aspect has receives less attention in the literature.

The overall objective of this study is to employ a newly developed high-resolution spatial (1.21 km2) and temporal (weekly) gridded dataset of drought indices to characterise drought events in Spain. Specifically, this study aims to i) apply the

10   extreme value theory to determine the best threshold and probability distribution to fit drought duration and magnitude probability, ii) explore spatial variations in this probability as a function of two common drought indices, with different underlying calculations (i.e. SPI vs. SPEI), and iii) assess whether there are spatial differences in drought hazard probability in response to using different drought timescales. In Spain, such detailed spatial assessment is still lacking, which limits the possibility to provide guidance on the use of drought hazard probability to manage and mitigate drought risks at the national,

15   regional and even local scale.


## 2 Data and methods

### 2.1 Dataset

We employed a high spatial resolution (1.21 km2) weekly drought dataset, spanning the period from 1961 to 2014 and covering the whole Spain. This dataset was developed based on gridded data of maximum and minimum air temperatures,

20   precipitation, wind speed, relative humidity and sunshine duration. The data were quality-controlled and subject to a careful homogenization assessment. Using these gridded data, we computed the Standardized Precipitation Index (SPI) (McKee et al., 1993) and the Standardized Precipitation Evapotranspiration Index (SPEI) (Vicente-Serrano et al., 2010). While the SPI accounts only for precipitation data, the SPEI is based on normalization of the climatic balance, i.e. the difference between precipitation and atmospheric evaporative demand (AED). In this study, we employed these two drought indices to account

25   for the possible effect of the AED on drought hazard probability in Spain. Data of these two drought indices are available at timescales from 1- to 48-month via http://monitordesequia.csic.es. A detailed description of this dataset and its development is outlined in Vicente-Serrano et al. ( 2017). Here, we used the SPI and SPEI at time scales of 1-, 3-, 6- and 12-months from 1961 to 2014, accounting for both meteorological and hydrological droughts.


### 2.2 Selection of drought events

30   Following the run theory (Guerrero-Salazar and Yevjevich, 1975; Moyé et al., 1988; Moyé and Kapadia, 1995; Yevjevich, 1967), there are several criteria to identify independent drought events based on thresholds (e.g. Fleig et al., 2006; Lee et al.,

Natural Hazards
and Earth System
Sciences
Discussions

1986). Nevertheless, these thresholds are generally arbitrary, as they do not rely on objective metrics that relate a certain value of a drought index to specific sectorial impacts. Indeed, this is a challenging task, given the large number of economic sectors and environmental systems impacted by droughts on one hand (Pérez and Barreiro-Hurlé, 2009), and the varying responses to different drought timescales among sectors and regions on the other hand (Lorenzo-Lacruz et al., 2013; Pasho et

5  al., 2012). In this work, we obtained the series of drought events from the weekly gridded series of the SPEI and the SPI at four selected time scales (1-, 3-, 6- and 12-months), using an arbitrary threshold equal to zero. Although this threshold allows for inclusion of drought events with low duration and magnitude, this criterion allows for securing larger sampling size for the probabilistic analysis, in comparison to using more restricted thresholds. Moreover, the retention of drought events with low duration and magnitude will not bias the results, given that high values of the series are those that are

10  retained following the peak-over-threshold approach.

Therefore, we defined each drought event as that event with a period of n consecutive weeks with SPI or SPEI values lower than zero. Once the drought events were identified, the series of drought duration and magnitude were created. The drought magnitude was calculated following the classical approach of Dracup et al. (1980), integrating the SPEI or SPI values over the drought period. However, it is noteworthy indicating that—for operative purposes—the total magnitude of drought was

15  transformed to positive values. In a similar manner, the drought duration was calculated for the consecutive weeks with SPEI or SPI values below zero.

## 2.3 Probabilistic analysis

We obtained the series of peaks-over-threshold (POT) using the series of drought duration and magnitude calculated at 1-, 3- , 6- and 12-month timescales. These series are stationary and do not show any trend (Domínguez-Castro et al., 2018), which

20  is a prerequisite to apply the extreme value theory. The POT series are obtained according to a threshold ($x_0$), as:

$$Y = X - x_0 \forall X > x_0 \tag{1}$$

Here, we tested different thresholds based on the centiles of the series (i.e. 0th, 10th, 20th,…, 90th and 95th), with the purpose of exploring the role of the selected threshold in fitting the probability distribution of the series. Following this procedure, we set the best centile threshold to define the exceedance series of drought duration and magnitude for the two

25  drought indices and the four timescales.

It has been widely demonstrated that the probability distribution of a POT series with random occurrence times fits well with GP distribution, as evidenced in many previous works (e.g. Hosking et al., 1987; Pham et al., 2014; Wang, 1991). As such, it has been extensively used for modelling low flows and meteorological droughts (e.g. Fleig et al., 2006; Liu et al., 2016; Nadarajah, 2008; Nadarajah and Kotz, 2008; Tošić and Unkašević, 2014; Yusof et al., 2013). The GP distribution is a

30  flexible, long-tailed distribution, whose distribution function is formulated, as:

$$F(x) = 1 - \left[1 - \frac{\kappa}{\alpha}(x - \varepsilon)\right]^{1/\kappa} \tag{2}$$

where κ, α and ε are the shape, scale and location parameters of the distribution origin that corresponds to the lower bound x0. The GP parameters were obtained using the L-moment statistics, according to (Hosking, 1990). This distribution has been widely used to obtain the quantile estimates of drought duration and magnitude series derived from drought indices in different world regions (e.g. Chen et al., 2011; Fleig et al., 2006; Tošić and Unkašević, 2014; Trenberth et al., 2014; Zamani

5   et al., 2015).

Hosking (1990) provided parametric approximations to the relationships between τ3 and τ4 (L-skewness and L-kurtosis respectively), which permit comparison with the ratio estimations, and determine the suitability of the GP distribution to fit the exceedance obtained from different x0 values. To determine the suitability of the different x0 thresholds to obtain POT series with good fitting to a GP distribution, we plotted the different L-moment diagrams with the statistics obtained from the

10  drought duration and magnitude series, as suggested by the SPI and SPEI as well as the four drought timescales.

We applied the Anderson-Darling test to check the goodness of fitting of the POT series, obtained from different x0 thresholds, to a GP distribution. Moreover, to select the most suitable threshold, we took into account the availability of a sample of sufficient length to obtain solutions for the GP parameters and accordingly reliable probabilistic estimations. For this purpose, we also compared the observed maximum drought duration and magnitude in the 54-yrs study period (1961-

15  2014) with the maximum estimates by means of the GP distribution and the POT series obtained from the different thresholds. We calculated the probability that an event of magnitude XT in a period of T = 54 years (expressed in the original scale) will occur at least once in a period of t years, according to:

$$\mathbf{X_T} = \boldsymbol{\varepsilon} + \frac{\alpha}{\kappa}\left[\mathbf{1} - \left(\frac{1}{\lambda T}\right)^{\kappa}\right]$$   (3)

where λ is a frequency parameter equalling the average number of occurrences of X per year in the original sample. The

20  performance of each threshold was assessed by means of different error/accuracy statistics. For this purpose, we used the mean absolute error (MAE), the Willmot' D agreement index (Willmott, 1981), and the Pearson's r correlation coefficient.

Once a general threshold was established to define the POT series of drought duration and magnitude for the two drought indices and the four drought time scales, we determined the goodness of the GP modelling. For this purpose, we used probability-probability (p-p) plots, which define the extent to which the empirical and modelled GP cumulative distribution

25  functions (cdfs) closely agree. This procedure was applied to 412,178 gridded series of drought magnitude and duration for the four time scales of the SPI and SPEI. Empirical cdfs were obtained using the plotting position formula proposed by Hosking (1990) for highly skewed data, written as:

$$P(X \leq x) = \frac{i - 0.35}{N}$$   (4)

where i is the rank of the observations arranged in descending order, and N is the number of observations. The goodness of

30  agreement between the empirical and modelled cdfs was determined by means of a weight correlation coefficient to give more importance to the highest, less-frequent observations in the sample, which are of more relevant to extreme values analysis. The weight was defined using the empirical cdf, as:

Natural Hazards
and Earth System
Sciences
Discussions

$$w_j = \frac{1}{1-cdf(j)} \text{w\_j} \qquad\qquad (5)$$

## 3 Results

### 3.1 Selection of the distribution and threshold to define the POT series

Figure 1 shows some examples of L-moment diagrams considering the 1-month SPEI duration series over the peninsular
5    Spain. The series for each diagram were obtained considering POT at different centiles. As illustrated, irrespective of the
threshold, the drought duration series tend to closely approximate to the GP distribution. Notably, there is a higher dispersion
of points around the theoretical curve at higher centiles; this is seen simply in the context of lower sampling size.
Nevertheless, the observed pattern of drought duration at 1-month timescale can be different considering other drought
timescales. Figure 2 depicts the L-moment diagrams corresponding to the 12-month SPEI magnitude series. The plots show
10   high dispersion considering the different centile thresholds. Nevertheless, at low centiles, the points do not approximate to
the theoretical curve of the GP distribution, but they conversely tend to approximate to the GP curve at centiles between 60th
and 80th. Again, the points exhibited high dispersion at upper centiles (mostly above the 85th).   An inspection of
Supplementary Fig. S1 to S14 suggests similar patterns for other timescales as well as for the drought duration and
magnitude series obtained using the SPI. Table 1 summarizes the percentage of the POT series that fit well with the GP
15   distribution following Anderson-Darling statistic. As listed, the series of drought magnitude show better fit to GP
distribution than those of drought duration. Notably, there are no considerable differences among the SPI and SPEI. By
contrast, we noted remarkable differences, as a function of drought timescale. We found that a high percentage of the series
obtained for low centiles does not fit to the GP distribution, while this fitting improves markedly for  all drought duration
and magnitude series when considering higher centiles (mostly above the 40th centile). The only exceptions are found for the
20   duration series at 1-month timescale for both the SPI and SPEI. Notably, the percentage of POT series that fit well with the
GP distribution is almost close to 100% for thresholds higher than the 80th centile. Overall, although these results suggest
choosing high centiles (e.g. 90th or 95th) to define the series of drought duration and magnitude, our decision was to define
these series using a threshold of 80th centile. This decision is motivated by the notion that L-moment statistics show high
dispersion at the most upper centiles on one hand and it is difficult to secure enough sampling size considering these upper
25   centiles on the other hand. Also, from a statistical point of view, it is difficult to define L-moment statistics and GP
parameters, particularly for long timescales (Fig. 3 and Table 2). Accordingly, it is reasonable to consider lower centiles for
making the probabilistic estimations. Our results demonstrate that the series of drought duration and magnitude obtained
using the 80th centile as a threshold mostly fit to a GP distribution and the majority of the series ($\approx$ 99%) show solutions for
the GP parameters. A comparison of the observations and estimations for the study period (1961-2014) also supports this
30   selection. Figure 4 summarizes the accuracy metrics (i.e. Willmott's D, MAE and Pearson's r coefficient), computed by
comparing the maximum observed and modelled drought duration and magnitude at the grid scale. Results are shown for the

four timescales and for the SPEI and SPI. We noted higher agreement between the maximum observed and predicted values of drought magnitude series, compared to drought duration series. For drought magnitude, the agreement is better considering higher centiles, particularly at the 80th centile. This pattern is clearly evident for the SPI and SPEI and the four timescales. Similar results are obtained using Pearson's r correlation, irrespective of the timescale and the drought index.

5   We also compared the empirical and the modelled cumulative distribution functions (cdfs) using GP distribution, considering the 80th centile POT series. Again, the comparisons were made at the pixel scale and considering the two drought indices and the different timescales. A representative example is shown in Fig. 5, for the grid point at 40ºN and 3ºW. As illustrated, there is a very good agreement between the empirical and the modelled cdfs, regardless of the drought index and the timescale. As depicted, low agreement is observed for long timescales (6- and 12-month). This is expected due to the low

10   sampling size at long timescales, in comparison to shorter timescales. Overall, the weight correlations between the empirical and GP distribution modelled cdfs show very high values (> 0.98) in all cases, which is reflected in the general pattern observed across the whole Spain. Figure 6 shows the spatial distribution of the weight correlations between the empirical and GP distribution modelled cdfs using the 80th centile POT series. At 1- and 3-month timescales, the correlations are almost close to 1 for the entire Spain, indicating that the selected scheme of the 80th centile and the GP distribution are highly

15   suitable to statistically model drought duration and magnitude in our study domain. At the 6- and 12-month timescales, the magnitude of correlations decreases, though being above 0.97 in most areas.

## 3.2 Mapping drought duration and magnitude

Figure 7 illustrates the spatial distribution of the GP parameters for the 80th centile drought duration series obtained from the SPI. As depicted, there are considerable spatial variations in the distribution of these parameters as a function of the drought

20   timescale, this is notably the case for all parameters (i.e. $x_0$, $\alpha$ and $\kappa$). These parameters show some similarities with those obtained using the SPEI (Fig. 8) and the drought magnitude series as well (Supplementary Fig. S15 and S16).

We mapped drought probability for the drought duration and magnitude series using the parameter maps and Eq. (3). Figure 9 shows the predicted maximum drought duration (in weeks) obtained from the 1-, 3-, 6- and 12-month SPEI series for a period of 50 and 100 years. Results suggest important spatial differences among drought timescales. For example, at the 1-

25   month timescale, the maximum duration occur in central areas of Spain, with more than 40 weeks of consecutive negative SPEI values. This spatial configuration is similar at the 3-month timescale, where central and southern areas of Spain experience longer duration. In northern Spain, the predicted maximum drought duration is half than that in central Spain. Nevertheless, the spatial patterns of drought probability differ markedly at the time scales of 6- and 12-month, with the maximum duration found in southeastern and southwestern regions, besides some regions in the north and northeast. The

30   spatial patterns found at the timescale of 12-month closely resemble those observed at 6-month timescale, suggesting a maximum drought duration (>180 months) in a period of 50 years over some regions in southeast and along the eastern Mediterranean coast. Considering the maximum drought duration in a period of 100 years, drought events are expected to extend further, mostly in southern Spain. Drought probability maps using the SPI show spatial patterns similar to those

observed by means of the SPEI (Fig. 10). Similar to the SPEI, there are noticeable spatial differences, which are strongly linked to the drought timescale. Figure 11 summarizes the relationship between the maximum drought duration of SPEI and SPI, considering 1-, 3-, 6- and 12-month timescale and periods of 50 and 100 years. For drought duration, the agreement between the SPI and SPEI is stronger considering long timescales. For timescales between 1 and 6 months, the SPEI tends to

5    record higher quantile estimates than the SPI. Nevertheless, at 12-month timescale, the differences in the quantile estimates between the two indices are clearly minimized. Quantile estimates of drought magnitude show similar spatial patterns, as compared to those identified for drought duration series (Supplementary Fig. S17 to S19).

## 4 Discussion and conclusions

We developed high-resolution extreme drought probability maps for Spain using two widely-recognized drought indices that

10    are comparable spatially and temporally: the Standardized precipitation Index (SPI) and the Standardized Precipitation Evapotranspiration Index (SPEI). Albeit with their similar conceptual background, they differ in their input variables necessary for calculation. While the SPI accounts only for precipitation data (McKee et al., 1993), the SPEI includes the atmospheric evaporative demand in its calculations (Vicente-Serrano et al., 2010). In this study, we computed these two drought indices at different timescales (1-, 3-, 6- and 12-month) to determine whether there are noticeable spatial differences

15    in the obtained drought hazard probabilities, as a function of the different timescales.

We assessed the suitability of the GP distribution to model drought duration and magnitude events. Results demonstrate that drought magnitude and duration series mostly fit well with a GP distribution, a finding that was confirmed in earlier drought assessment investigations in many regions worldwide (e.g. Chen et al., 2011; Serra et al., 2016; Vicente-Serrano and Beguería-Portugués, 2003; Zamani et al., 2015). In this study, our decision was made to make balance between the goodness

20    of the fit to the GP distribution and the selection of a representative threshold to obtain the POT series. Our exploratory analysis suggests the use of the 80th centile as a threshold, which makes a good balance between the two requirements for the SPI and SPEI and for all timescales.

Numerous studies have followed a regionalization approach to estimate the probability distribution, L-moment statistics and the distribution parameters corresponding to hydrologic and climatic hazards including droughts (e.g. Durrans and Tomic,

25    1996; Serra et al., 2016; She et al., 2014). As opposed to these studies, our preference was given to analyse hazard probability locally. Specifically, in our calculation of the L-moment statistics and the distribution parameters, we considered each gridded cell as an independent series. While regionalization is advantageous in terms of spatial homogeneity and the reduction of the parameter uncertainty (Hosking and Wallis, 1997), quantifying drought conditions reveals noticeable spatial differences in our study domain, as a function of the drought time scale. This is clearly evident for probabilities of drought

30    duration and magnitude. Regionalization is usually based on the variables used for calculating drought indices (i.e. precipitation or climate balance) (Ghosh and Srinivasan, 2016; Habibi et al., 2018; Santos et al., 2011; Yuan et al., 2013; Zhang et al., 2015). Importantly, this study stresses that this kind of regionalization might not be useful when the drought

hazard differs strongly as a function of the drought timescale. Previous studies indicated that spatial patterns of drought may strongly differ as a function of the drought timescale, especially with the different temporal influence of local/regional precipitation events on drought index values (e.g. Vicente-Serrano 2006). This is confirmed in our study for the whole Spain, where the spatial patterns of the GP distribution and the maps of hazard probability strongly vary as a function of the drought

5    timescale. Again, this stresses the difficulty of applying regionalization approaches to obtain maps of drought probability. This difficulty is also enhanced by our findings on the spatial differences in the drought probability in response to the selected drought index. All together makes this kind of regionalization a challenging task. A possible solution could be establishing different regionalization schemes based on the different series of drought indices and timescales. However, this seems to be practically disadvantageous, with strong confusion for the use of probability estimations by end-users (e.g.

10   stakeholders, decision makers and local communities). Also, with the spatial coherence and the observed gradients of GP parameters, a direct calculation of hazard probabilities locally is highly recommended, particularly in regions with strong spatial and temporal climatic variability like Spain. Overall, taken all these limitations into consideration, it is recommended to avoid employing regionalization approaches to determine drought hazard probabilities when different drought indices and timescales are used.

15   Assessing the different spatial patterns of drought probabilities as a function of timescales has strong implications for drought impact assessment and drought mitigation, as it is well-established that different hydrological, agricultural and environmental systems respond differently to drought timescales (Pasho et al., 2012; Peña-Gallardo et al., 2018; Vicente-Serrano, 2013). For more effective assessment and monitoring of drought hazard, drought timescales must be linked with specific drought impacts. This is basically because although drought probability may differ as a function of drought

20   timescale, the impacts of drought hazard can vary considerably from one region to another in response to different environmental and socioeconomic factors. As such, the degree of vulnerability can vary according to drought timescale. For example, albeit with the high probability of occurrence of an extreme drought event at a certain timescale in a particular region, drought risk may be small if the sensitivity to drought timescale is low. This confirms that it is essential to obtain drought hazard probability maps at different timescales, given that the real hazard would be definitely derived from drought

25   timescale that triggers impacts in a given space and sector.

In recent years there is a great debate on the influence of climate change processes on drought severity (Dai, 2013; Sheffield et al., 2012; Trenberth et al., 2014). This debate is mainly motivated by the role of warming processes and the atmospheric evaporative demand (AED) in drought severity. Numerous studies have shown a noticeable increase in the AED across the Mediterranean region, which could enhance the severity of drought events in comparison to those events caused mainly by

30   precipitation deficit (Stagge et al., 2017; Vicente-Serrano et al., 2014). Here, we indicated that, mainly at timescales from 1- to 6-month, SPEI duration and magnitude values are higher than those of the SPI, suggesting that increased AED due to warming processes may have certain role in increasing drought duration and magnitude hazard probabilities in Spain. This indicates that when a drought occurs as a consequence of a precipitation deficit, high values of the AED may increase the magnitude and duration of drought events. Nevertheless, this pattern was not observed with long drought timescales (i.e. 12

month), which showed small differences between the SPI and SPEI drought duration and magnitude quantile maps. This could be explained by the strong seasonality that characterises the climate of Spain, given that the 12-month timescale summarizes the entire annual climate conditions. The role of increased AED (mostly recorded during summer months Vicente-Serrano et al. (2014)) would be diminished in comparison to the role of precipitation. In contrast, the role of the

5　AED would be well-recognized at shorter timescales that record seasonal variability.

In recent years, the study of drought hazard probability by means of joint probabilities of drought duration and magnitude has been applied in more depth by means of the use of copulas (e.g. Ganguli and Reddy, 2012; Liu et al., 2011; Zhang et al., 2015). Nevertheless, given the nature of the drought indices, time series show strong temporal autocorrelation and the duration and magnitude of particular drought events show high agreement. Here, we found a strong correlation between the

10　magnitude and the duration of drought events for the two used drought indices and the different drought timescales. This indicates that—as expected—the total magnitude of an event is proportional to drought duration, exhibiting similar spatial patterns of drought hazard probability either for drought duration or magnitude series. Therefore, although copulas could give some additional information for particular events, we still believe that an accurate evaluation of drought hazard probability in Spain using a univariate approach is adequate.

15　Given the strong spatial differences in the drought hazard probability over our study domain, the maps obtained in this study can be useful to improve the management of different sectors, including agriculture, water resources management, urban water supply, tourism and environmental management. The spatial quantile probabilities developed in this study and used to develop the 50 and 100 years quantile maps are fully available via the web repository of the Spanish National Research Council (CSIC) at https://digital.csic.es/.

20　**Author contribution**

All the authors contributed equally to the manuscript.

**Competing interests**

The authors declare that they have no conflict of interest.

**Acknowledgements**

Natural Hazards
and Earth System
Sciences
Discussions

# References

Chen, L.-H., Hong, Y.-T. and Hsu, C.-W.: A study on regional drought frequency analysis using self-organizing map and l-
5   moments, J. Taiwan Agric. Eng., 57(2), 57–77, 2011.

Dai, A.: Increasing drought under global warming in observations and models, Nat. Clim. Chang., 3(1), 52–58,
doi:10.1038/nclimate1633, 2013.

Domínguez-Castro, F., Vicente-Serrano, S. M., Tomás-Burguera, M., Peña-Gallardo, M., Beguería, S., El Kenawy, A., Luna,
Y. and Morata, A.: High spatial resolution climatology of drought events for Spain: 1961-2014, Int. J. Climatol., under
10  review, 2018.

Dracup, J. A., Lee, K. S. and Paulson, E. G.: On the definition of droughts, Water Resour. Res., 16(2), 297–302,
doi:10.1029/WR016i002p00297, 1980.

Durrans, S. R. and Tomic, S.: Regionalization of low-flow frequency estimates: An Alabama case study, J. Am. Water
Resour. Assoc., 32(1), 23–37, 1996.

15  Engeland, K., Hisdal, H. and Frigessi, A.: Practical extreme value modelling of hydrological floods and droughts: A case
study, Extremes, 7(1), 5–30, doi:10.1007/s10687-004-4727-5, 2005.

Fernández, A.: El sistema español de seguros agrarios, El Sect. Asegur. y los planes y fondos pensiones, 833, 87–99, 2006.

Fleig, A. K., Tallaksen, L. M., Hisdal, H. and Demuth, S.: A global evaluation of streamflow drought characteristics, Hydrol.
Earth Syst. Sci., 10(4), 535–552, doi:10.5194/hess-10-535-2006, 2006.

20  Ganguli, P. and Reddy, M. J.: Risk Assessment of Droughts in Gujarat Using Bivariate Copulas, Water Resour. Manag.,
26(11), 3301–3327, doi:10.1007/s11269-012-0073-6, 2012.

Garrick, D. E., Hall, J. W., Dobson, A., Damania, R., Grafton, R. Q., Hope, R., Hepburn, C., Bark, R., Boltz, F., De Stefano,
L., O'Donnell, E., Matthews, N. and Money, A.: Valuing water for sustainable development, Science, 358(6366), 1003–
1005, doi:10.1126/science.aao4942, 2017.

25  Ghosh, S. and Srinivasan, K.: Analysis of Spatio-temporal Characteristics and Regional Frequency of Droughts in the
Southern Peninsula of India, Water Resour. Manag., 30(11), 3879–3898, doi:10.1007/s11269-016-1396-5, 2016.

González-Hidalgo, J. C., Vicente-Serrano, S. M., Peña-Angulo, D., Salinas, C., Tomas-Burguera, M. and Beguería, S.: High-
resolution spatio-temporal analyses of drought episodes in the western Mediterranean basin (Spanish mainland, Iberian
Peninsula), Acta Geophys., 66, 381–392, 2018.

30  Guerrero-Salazar, P. and Yevjevich, V. .: Analysis of drought characteristics by the theory of runs, Hydrol. Pap. Color. State
Univ., 80, 1–44, 1975.

Habibi, B., Meddi, M., Torfs, P. J. J. F., Remaoun, M. and Van Lanen, H. A. J.: Characterisation and prediction of

meteorological drought using stochastic models in the semi-arid Chéliff–Zahrez basin (Algeria), J. Hydrol. Reg. Stud., 16, 15–31, doi:10.1016/j.ejrh.2018.02.005, 2018.

Hosking, J. R. . and Wallis, J. R.: Regional Frequency Analysis: An Approach Based on L-moments, Cambridge University Press., 1997.

5   Hosking, J. R. M.: L-moments: analysis and estimation of distributions using linear combinations of order statistics, J R Stat Soc Ser. B Stat Methodol, 52, 105–124, 1990.

Hosking, J. R. M., Wallis, J. R. and Hosking, J. R. M.: Parameter and quantile estimation for the generalized pareto distribution, Technometrics, 29(3), 339–349, doi:10.1080/00401706.1987.10488243, 1987.

Hussain, T., Bakouch, H. S. and Iqbal, Z.: A New Probability Model for Hydrologic Events: Properties and Applications, J.

10   Agric. Biol. Environ. Stat., 23(1), 63–82, doi:10.1007/s13253-017-0313-6, 2018.

Lana, X., Martínez, M. D., Burgueño, A., Serra, C., Martín-Vide, J. and Gómez, L.: Distributions of long dry spells in the Iberian Peninsula, years 1951-1990, Int. J. Climatol., 26(14), 1999–2021, doi:10.1002/joc.1354, 2006.

Lee, K. S., Sadeghipour, J. and Dracup, J. A.: An Approach for Frequency Analysis of Multiyear Drought Durations, Water Resour. Res., 22(5), 655–662, doi:10.1029/WR022i005p00655, 1986.

15   Liu, C.-L., Zhang, Q., Singh, V. P. and Cui, Y.: Copula-based evaluations of drought variations in Guangdong, South China, Nat. Hazards, 59(3), 1533–1546, doi:10.1007/s11069-011-9850-4, 2011.

Liu, Y., Lu, M., Huo, X., Hao, Y., Gao, H., Liu, Y., Fan, Y., Cui, Y. and Metivier, F.: A Bayesian analysis of Generalized Pareto Distribution of runoff minima, Hydrol. Process., 30(3), 424–432, doi:10.1002/hyp.10606, 2016.

Lorenzo-Lacruz, J., Morán-Tejeda, E., Vicente-Serrano, S. M. and López-Moreno, J. I.: Streamflow droughts in the Iberian

20   Peninsula between 1945 and 2005: Spatial and temporal patterns, Hydrol. Earth Syst. Sci., 17(1), 119–134, doi:10.5194/hess-17-119-2013, 2013.

Maia, R. and Vicente-Serrano, S. M.: Drought planning and management in the iberian peninsula, in: Drought and Water Crises, CRC Press, Boca Raton, 481-506, 2017.

Martin-Vide, J. and Gomez, L.: Regionalization of peninsular Spain based on the length of dry spells, Int. J. Climatol., 19(5),

25   537–555, 1999.

McKee, T. B., Doesken, N. J. and Kleist, J.: The relationship of drought frequency and duration to time scales, Eighth Conf. Appl. Climatol., 179–184, 1993.

Mishra, A. K. and Singh, V. P.: Drought modeling - A review, J. Hydrol., 403(1–2), 157–175, doi:10.1016/j.jhydrol.2011.03.049, 2011.

30   Mishra, A. K., Singh, V. P. and Desai, V. R.: Drought characterization: A probabilistic approach, Stoch. Environ. Res. Risk Assess., 23(1), 41–55, doi:10.1007/s00477-007-0194-2, 2009.

Moradi, H. R., Rajabi, M. and Faragzadeh, M.: Investigation of meteorological drought characteristics in Fars province, Iran, Catena, 84(1–2), 35–46, doi:10.1016/j.catena.2010.08.016, 2011.

Moyé, L. A. and Kapadia, A. S.: Predictions of drought length extreme order statistics using run theory, J. Hydrol., 169(1–4),

95–110, doi:10.1016/0022-1694(94)02662-U, 1995.

Moyé, L. A., Kapadia, A. S., Cech, I. M. and Hardy, R. J.: The theory of runs with applications to drought prediction, J. Hydrol., 103(1–2), 127–137, doi:10.1016/0022-1694(88)90010-8, 1988.

Nadarajah, S.: Generalized Pareto models with application to drought data, Environmetrics, 19(4), 395–408, doi:10.1002/env.885, 2008.

Nadarajah, S. and Kotz, S.: The generalized Pareto sum, Hydrol. Process., 22(2), 288–294, doi:10.1002/hyp.6602, 2008.

Pasho, E., Camarero, J. J. and Vicente-Serrano, S. M.: Climatic impacts and drought control of radial growth and seasonal wood formation in Pinus halepensis, Trees - Struct. Funct., 26(6), 1875–1886, doi:10.1007/s00468-012-0756-x, 2012.

Peña-Gallardo, M., Vicente-Serrano, S. M., Domínguez-Castro, F., Quiring, S., Svoboda, M., Beguería, S. and Hannaford, J.: Effectiveness of drought indices in identifying impacts on major crops across the USA, Clim. Res., 75(3), 221–240, 2018.

Pérez-Sánchez, J. and Senent-Aparicio, J.: Analysis of meteorological droughts and dry spells in semiarid regions: a comparative analysis of probability distribution functions in the Segura Basin (SE Spain), Theor. Appl. Climatol., 133(3–4), 1061–1074, doi:10.1007/s00704-017-2239-x, 2018.

Pérez, L. and Barreiro-Hurlé, J.: Assessing the socio-economic impacts of drought in the Ebro River Basin | Análisis de los efectos socioeconómicos de la sequía en la cuenca del Ebro, Spanish J. Agric. Res., 7(2), 269–280, 2009.

Pham, H. X., Asaad, Y. and Melville, B.: Statistical properties of partial duration series: Case study of North Island, New Zealand, J. Hydrol. Eng., 19(4), 807–815, doi:10.1061/(ASCE)HE.1943-5584.0000841, 2014.

Redmond, K. T.: The depiction of drought: A commentary, Bull. Am. Meteorol. Soc., 83(8), 1143–1147, doi:10.1175/1520-0477(2002)083<1143:TDODAC>2.3.CO;2, 2002.

Santos, J. F., Portela, M. M. and Pulido-Calvo, I.: Regional Frequency Analysis of Droughts in Portugal, Water Resour. Manag., 25(14), 3537–3558, doi:10.1007/s11269-011-9869-z, 2011.

Serra, C., Lana, X., Burgueño, A. and Martínez, M. D.: Partial duration series distributions of the European dry spell lengths for the second half of the twentieth century, Theor. Appl. Climatol., 123(1–2), 63–81, doi:10.1007/s00704-014-1337-2, 2016.

She, D.-X., Xia, J., Zhang, D., Ye, A.-Z. and Sood, A.: Regional extreme-dry-spell frequency analysis using the L-moments method in the middle reaches of the Yellow River Basin, China, Hydrol. Process., 28(17), 4694–4707, doi:10.1002/hyp.9930, 2014.

Sheffield, J., Wood, E. F. and Roderick, M. L.: Little change in global drought over the past 60 years, Nature, 491(7424), 435–438, doi:10.1038/nature11575, 2012.

Stagge, J. H., Kingston, D. G., Tallaksen, L. M. and Hannah, D. M.: Observed drought indices show increasing divergence across Europe, Sci. Rep., 7(1), doi:10.1038/s41598-017-14283-2, 2017.

Svoboda, M., LeComte, D., Hayes, M., Heim, R., Gleason, K., Angel, J., Rippey, B., Tinker, R., Palecki, M., Stooksbury, D., Miskus, D. and Stephens, S.: The drought monitor, Bull. Am. Meteorol. Soc., 83(8), 1181–1190, doi:10.1175/1520-0477(2002)083<1181:TDM>2.3.CO;2, 2002.

Tošić, I. and Unkašević, M.: Analysis of wet and dry periods in Serbia, Int. J. Climatol., 34(5), 1357–1368, doi:10.1002/joc.3757, 2014.

Tosunoglu, F. and Can, I.: Application of copulas for regional bivariate frequency analysis of meteorological droughts in Turkey, Nat. Hazards, 82(3), 1457–1477, doi:10.1007/s11069-016-2253-9, 2016.

5    Trenberth, K. E., Dai, A., Van Der Schrier, G., Jones, P. D., Barichivich, J., Briffa, K. R. and Sheffield, J.: Global warming and changes in drought, Nat. Clim. Chang., 4(1), 17–22, doi:10.1038/nclimate2067, 2014.

UNEP: Geo Year Book 2006: An overview of our changing environment, Nairobi., 2006.

Vicente-Serrano, S. M.: Differences in spatial patterns of drought on different time scales: An analysis of the Iberian Peninsula, Water Resour. Manag., 20(1), 37–60, doi:10.1007/s11269-006-2974-8, 2006.

10   Vicente-Serrano, S. M.: Spatial and temporal evolution of precipitation droughts in Spain in the last century, in Adverse Weather in Spain, edited by F. Martínez, CC-L., Rodríguez, pp. 283–296., 2013.

Vicente-Serrano, S. M. and Beguería-Portugués, S.: Estimating extreme dry-spell risk in the middle Ebro valley (northeastern Spain): A comparative analysis of partial duration series with a general Pareto distribution and annual maxima series with a Gumbel distribution, Int. J. Climatol., 23(9), 1103–1118, doi:10.1002/joc.934, 2003.

15   Vicente-Serrano, S. M., Beguería, S. and López-Moreno, J. I.: A multiscalar drought index sensitive to global warming: The standardized precipitation evapotranspiration index, J. Clim., 23(7), 1696–1718, doi:10.1175/2009JCLI2909.1, 2010.

Vicente-Serrano, S. M., Azorin-Molina, C., Sanchez-Lorenzo, A., Revuelto, J., López-Moreno, J. I., González-Hidalgo, J. C., Moran-Tejeda, E. and Espejo, F.: Reference evapotranspiration variability and trends in Spain, 1961-2011, Glob. Planet. Change, 121, 26–40, doi:10.1016/j.gloplacha.2014.06.005, 2014.

20   Vicente-Serrano, S. M., Tomas-Burguera, M., Beguería, S., Reig, F., Latorre, B., Peña-Gallardo, M., Luna, M. Y., Morata, A. and González-Hidalgo, J. C.: A High Resolution Dataset of Drought Indices for Spain, Data, 2(3), 22, doi:10.3390/data2030022, 2017.

Wang, Q. J.: The POT model described by the generalized Pareto distribution with Poisson arrival rate, J. Hydrol., 129(1–4), 263–280, doi:10.1016/0022-1694(91)90054-L, 1991.

25   Wilhite, D. and Pulwarty, R. S.: Drought and Water Crises: Integrating Science, Management, and Policy, CRC Press, Boca Raton., 2017.

Willmott, C. J.: On the validation of models, Phys. Geogr., 2(2), 184–194, doi:10.1080/02723646.1981.10642213, 1981.

Yan, G., Wu, Z., Li, D. and Xiao, H.: A comparative frequency analysis of three standardized drought indices in the poyang lake basin, china, Nat. Hazards, 91(1), 353–374, doi:10.1007/s11069-017-3133-7, 2018.

30   Yevjevich, V. M.: An objective approach to definition and investigation of continental hydrologic droughts., 1967.

Yuan, X.-C., Zhou, Y.-L., Jin, J.-L. and Wei, Y.-M.: Risk analysis for drought hazard in China: A case study in Huaibei Plain, Nat. Hazards, 67(2), 879–900, doi:10.1007/s11069-013-0614-1, 2013.

Yusof, F., Hui-Mean, F., Suhaila, J. and Yusof, Z.: Characterisation of Drought Properties with Bivariate Copula Analysis, Water Resour. Manag., 27(12), 4183–4207, doi:10.1007/s11269-013-0402-4, 2013.

Zamani, R., Tabari, H. and Willems, P.: Extreme streamflow drought in the Karkheh river basin (Iran): probabilistic and regional analyses, Nat. Hazards, 76(1), 327–346, doi:10.1007/s11069-014-1492-x, 2015.

Zhang, Q., Qi, T., Singh, V. P., Chen, Y. D. and Xiao, M.: Regional Frequency Analysis of Droughts in China: A Multivariate Perspective, Water Resour. Manag., 29(6), 1767–1787, doi:10.1007/s11269-014-0910-x, 2015.

5   Zin, W. Z. W., Jemain, A. A. and Ibrahim, K.: Analysis of drought condition and risk in Peninsular Malaysia using Standardised Precipitation Index, Theor. Appl. Climatol., 111(3–4), 559–568, doi:10.1007/s00704-012-0682-2, 2013.

**Table 1 Percentage of the peaks-over-threshold drought duration and magnitude series that fit well with the Generalized Pareto distribution following Anderson-Darling statistic. Results are summarized for different centiles and timescales using SPEI and SPI.**

| | Magnitude | | | | Duration | | | |
|---|---|---|---|---|---|---|---|---|
| SPEI | 1-month | 3-month | 6-month | 12-month | 1-month | 3-month | 6-month | 12-month |
| 00th | 98.5 | 42.8 | 51.8 | 68.9 | 0.0 | 12.8 | 51.7 | 81.6 |
| 10th | 100.0 | 91.1 | 90.4 | 91.5 | 3.8 | 91.0 | 98.3 | 99.2 |
| 20th | 100.0 | 99.8 | 99.1 | 98.4 | 3.8 | 94.8 | 99.1 | 99.6 |
| 30th | 100.0 | 100.0 | 100.0 | 99.9 | 5.6 | 99.5 | 99.9 | 99.9 |
| 40th | 100.0 | 100.0 | 100.0 | 100.0 | 8.9 | 100.0 | 100.0 | 100.0 |
| 50th | 100.0 | 100.0 | 100.0 | 100.0 | 37.0 | 100.0 | 100.0 | 100.0 |
| 60th | 100.0 | 100.0 | 100.0 | 100.0 | 57.9 | 100.0 | 100.0 | 100.0 |
| 70th | 100.0 | 100.0 | 100.0 | 100.0 | 84.3 | 100.0 | 100.0 | 100.0 |
| 80th | 100.0 | 100.0 | 100.0 | 100.0 | 98.6 | 100.0 | 100.0 | 100.0 |
| 90th | 100.0 | 100.0 | 100.0 | 100.0 | 98.8 | 100.0 | 100.0 | 100.0 |
| 95th | 100.0 | 100.0 | 100.0 | 96.9 | 98.6 | 100.0 | 99.9 | 98.5 |
| SPI | 1-month | 3-month | 6-month | 12-month | 1-month | 3-month | 6-month | 12-month |
| 00th | 85.8 | 27.9 | 41.3 | 70.9 | 0.0 | 6.4 | 39.2 | 81.5 |
| 10th | 99.3 | 79.9 | 80.8 | 88.9 | 0.1 | 84.4 | 96.8 | 99.1 |
| 20th | 100.0 | 99.0 | 97.3 | 97.3 | 0.1 | 89.8 | 98.2 | 99.5 |
| 30th | 100.0 | 100.0 | 99.9 | 99.7 | 1.4 | 98.0 | 99.8 | 99.9 |
| 40th | 100.0 | 100.0 | 100.0 | 100.0 | 5.0 | 99.8 | 100.0 | 100.0 |
| 50th | 100.0 | 100.0 | 100.0 | 100.0 | 20.8 | 100.0 | 100.0 | 100.0 |
| 60th | 100.0 | 100.0 | 100.0 | 100.0 | 45.2 | 100.0 | 100.0 | 100.0 |
| 70th | 100.0 | 100.0 | 100.0 | 100.0 | 75.7 | 100.0 | 100.0 | 100.0 |
| 80th | 100.0 | 100.0 | 100.0 | 100.0 | 94.4 | 100.0 | 100.0 | 100.0 |
| 90th | 100.0 | 100.0 | 100.0 | 100.0 | 98.6 | 100.0 | 100.0 | 99.9 |
| 95th | 100.0 | 100.0 | 100.0 | 98.2 | 97.1 | 99.9 | 99.9 | 98.8 |

5

**Table 2 Percentage of cases in which solution for the L-moment and the Generalized Pareto distribution parameters is found for the peaks over threshold drought duration/magnitude series at different centiles from 1-, 3-, 6-, and 12-month SPI and SPEI.**

|  | 1-month SPEI | 3-month SPEI | 6-month SPEI | 12-month SPEI | 1-month SPI | 3-month SPI | 6-month SPI | 12-month SPI |
|---|---|---|---|---|---|---|---|---|
| 00th | 100.0 | 100.0 | 100.0 | 100.0 | 100.0 | 100.0 | 100.0 | 100.0 |
| 10th | 100.0 | 100.0 | 100.0 | 100.0 | 100.0 | 100.0 | 100.0 | 100.0 |
| 20th | 100.0 | 100.0 | 100.0 | 100.0 | 100.0 | 100.0 | 100.0 | 100.0 |
| 30th | 100.0 | 100.0 | 100.0 | 100.0 | 100.0 | 100.0 | 100.0 | 100.0 |
| 40th | 100.0 | 100.0 | 100.0 | 100.0 | 100.0 | 100.0 | 100.0 | 100.0 |
| 50th | 100.0 | 100.0 | 100.0 | 100.0 | 100.0 | 100.0 | 100.0 | 100.0 |
| 60th | 100.0 | 100.0 | 100.0 | 100.0 | 100.0 | 100.0 | 100.0 | 99.9 |
| 70th | 100.0 | 100.0 | 100.0 | 99.6 | 100.0 | 100.0 | 99.9 | 99.2 |
| 80th | 100.0 | 100.0 | 99.7 | 97.4 | 100.0 | 99.9 | 99.3 | 96.8 |
| 90th | 99.7 | 98.5 | 96.8 | 79.8 | 99.5 | 97.7 | 96.6 | 84.9 |
| 95th | 98.7 | 86.7 | 75.9 | 52.7 | 96.8 | 91.1 | 85.0 | 52.8 |

5

Natural Hazards
and Earth System
Sciences

Open Access

Discussions

EGU
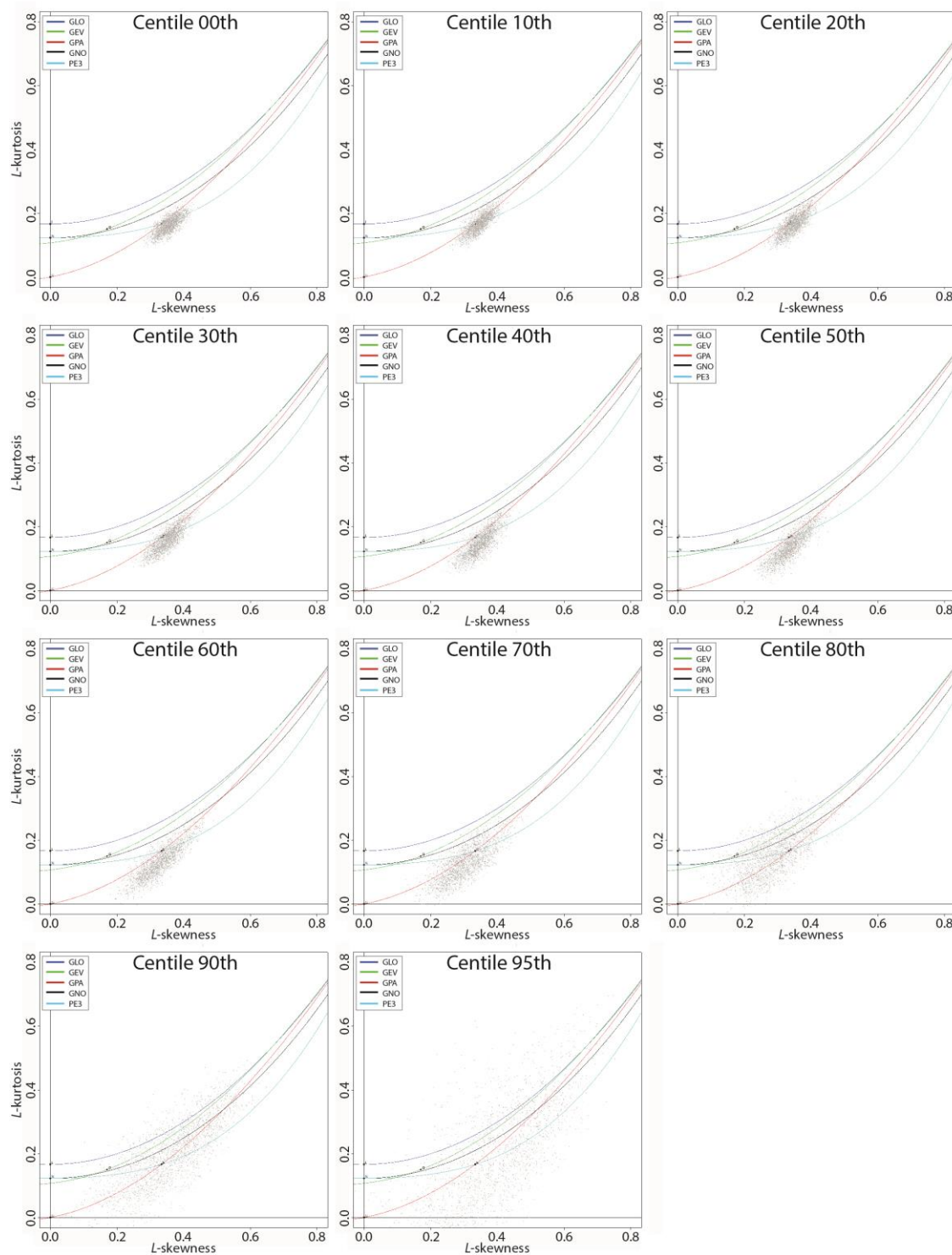


**Figure 1: L-moment diagrams for the peak-over-threshold series obtained from the 1-month SPEI duration series.**
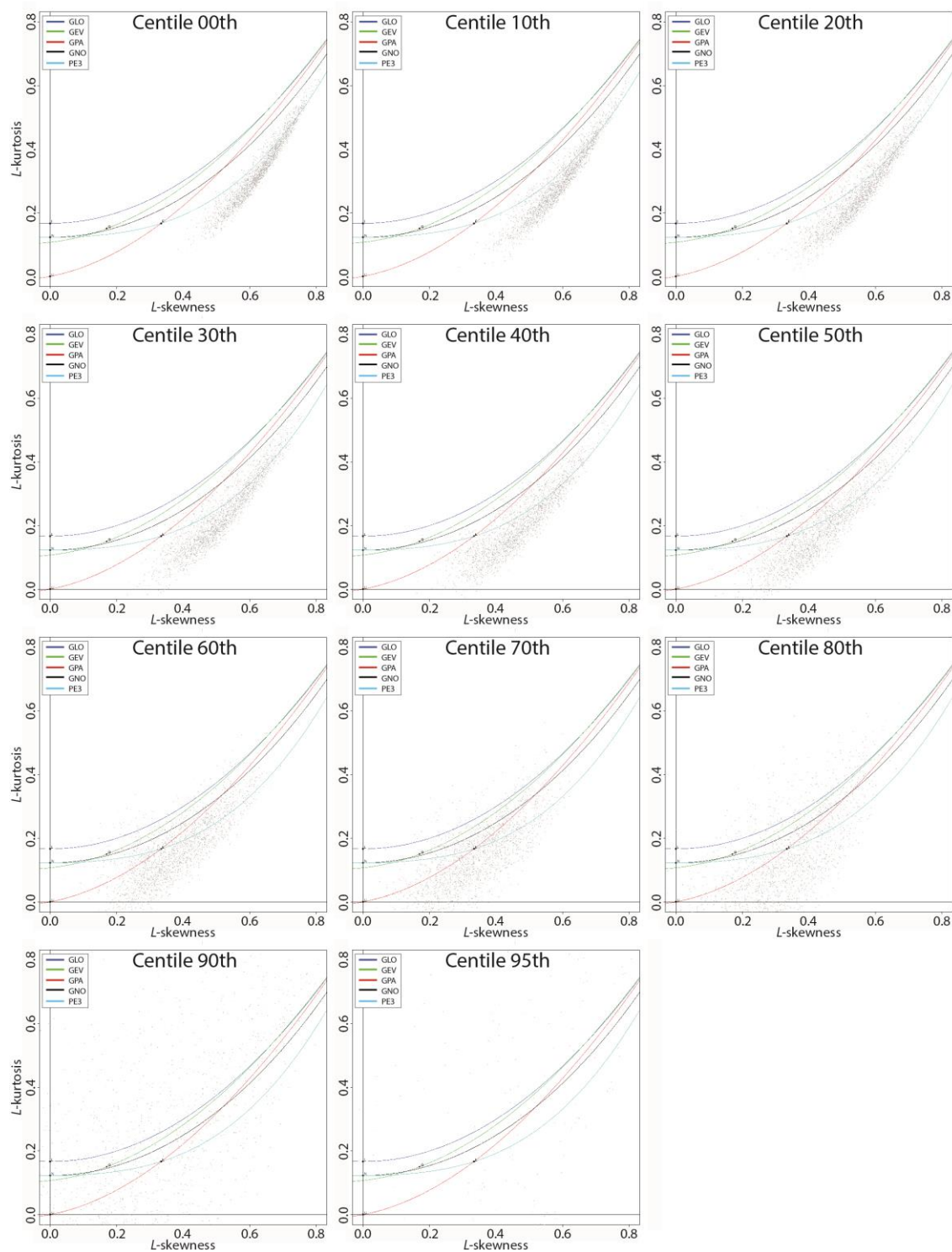
**Figure 2: L-moment diagrams for the peak-over-threshold series obtained from the 12-month SPEI magnitude series.**

**Figure 3: Probability density diagrams showing the number of cases corresponding to the peaks over threshold drought duration/magnitude series at different centiles and different timescales (1-, 3-, 6-, and 12-month) using (a) SPI and (b) SPEI.**

5

Natural Hazards
and Earth System
Sciences

Open Access

Discussions

EGU
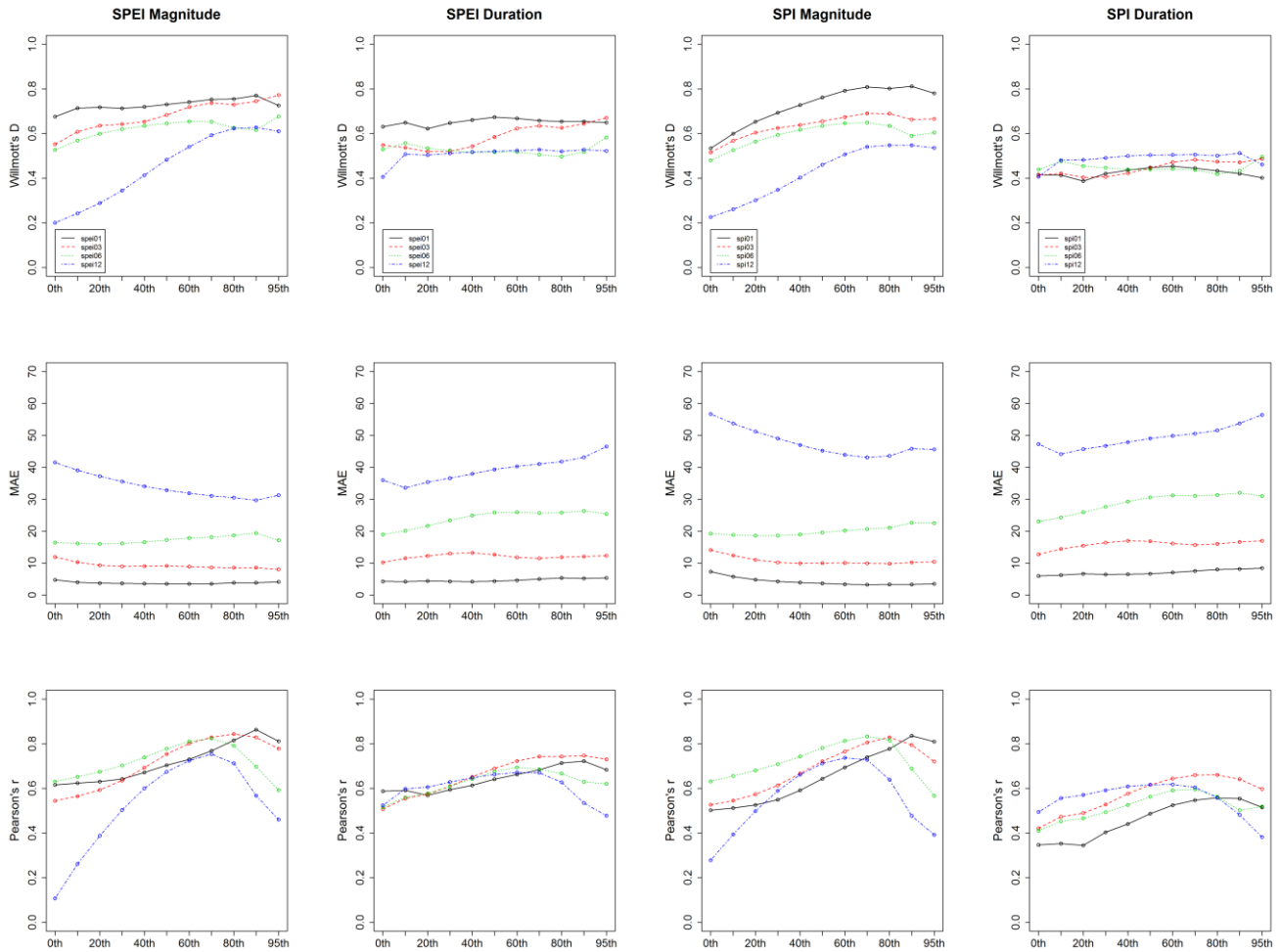


**Figure 4: Willmott's D, mean absolute error (MAE) and Pearson's r, summarized as a function of the different centiles used to obtain the peaks-over-threshold series. All accuracy metrics were computed based on comparing the maximum observed and modelled 1-, 3-, 6- and 12-month SPI and SPEI drought duration and magnitude between 1961 and 2014. The modelled data were computed using the Generalized Pareto distribution.**
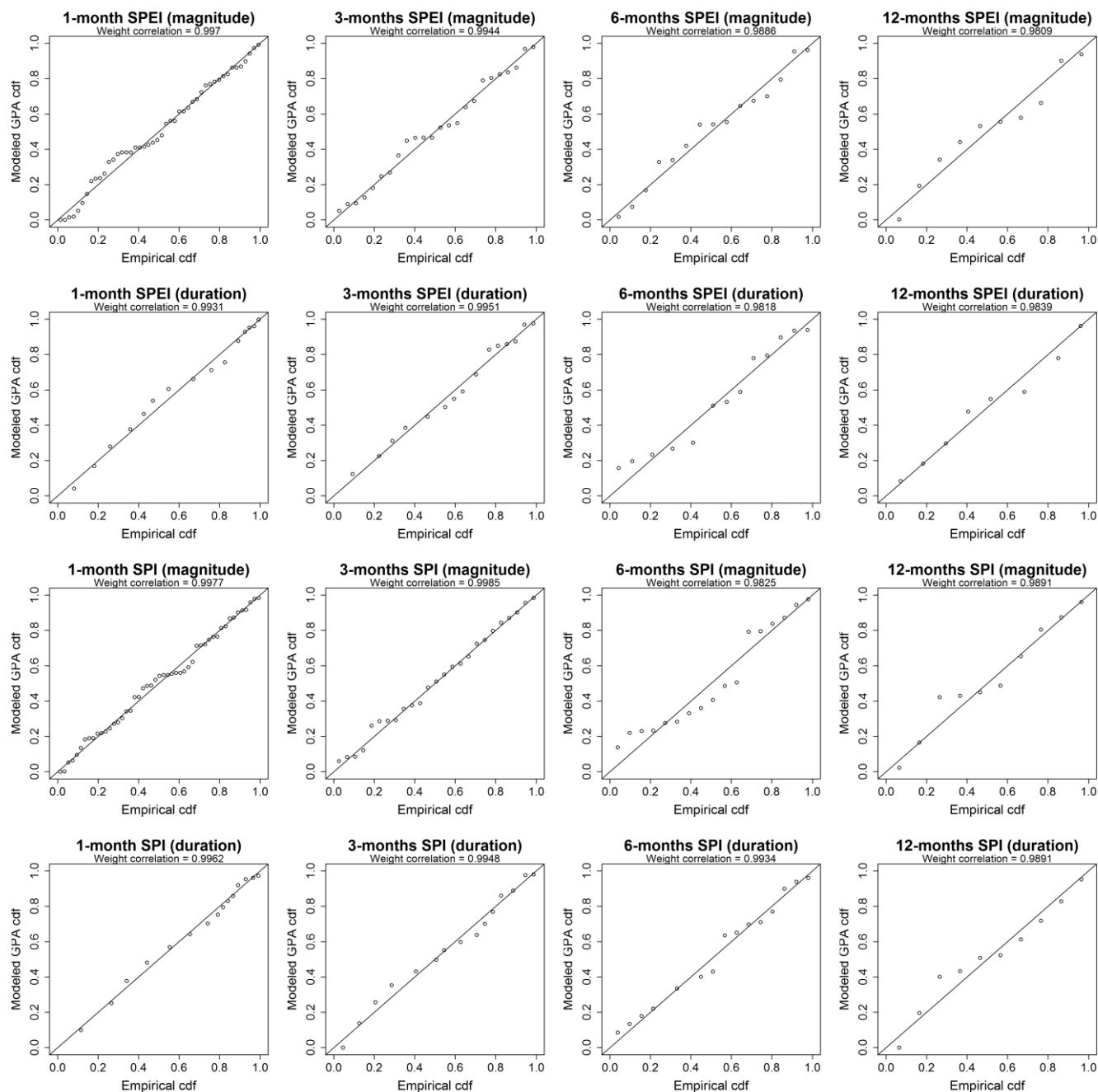
**Figure 5: Example of probability-probability (P-P) plots for the series of 1-, 3-, 6- and 12-month SPEI and SPI drought duration and drought magnitude obtained by means of the 80$^{th}$ centile used as a threshold to derive the peak-over-threshold series.**
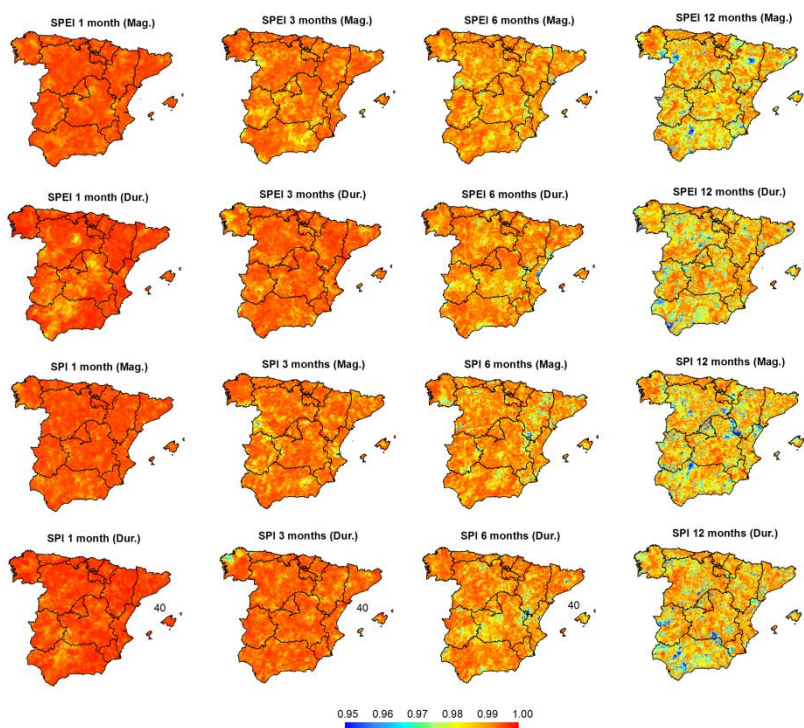
**Figure 6: Spatial distribution of the weight correlation coefficients from probability-probability (P-P) plots from the series of 1-, 3-, 6- and 12-month SPEI and SPI drought duration and magnitude series obtained considering the 80th centile as a threshold for the peak-over-threshold series.**

5

Natural Hazards
and Earth System
Sciences
Discussions
Open Access
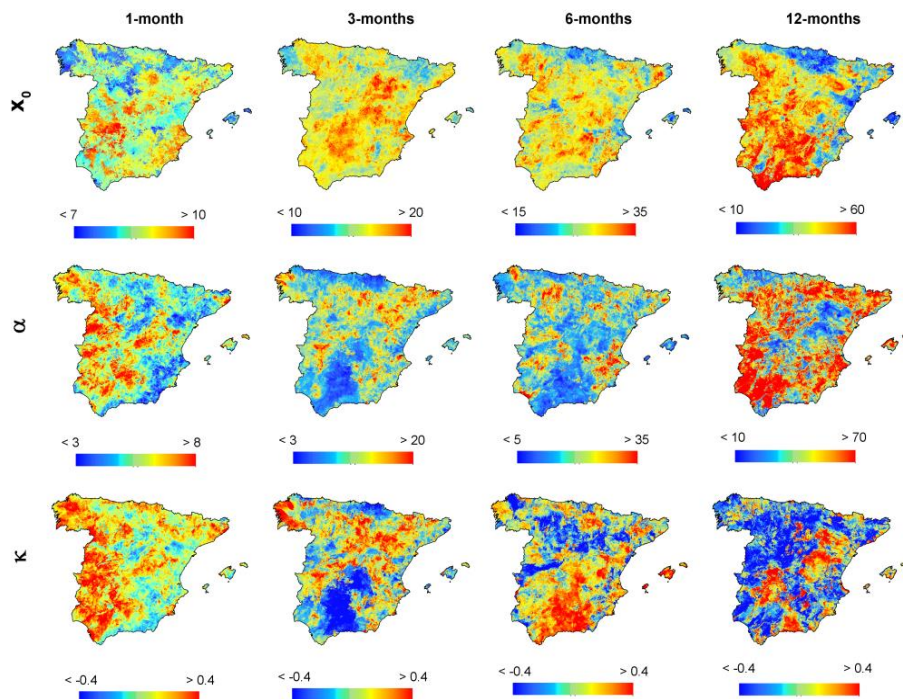


Figure 7: Spatial distribution of the parameters of the GP distribution for the SPI duration series.
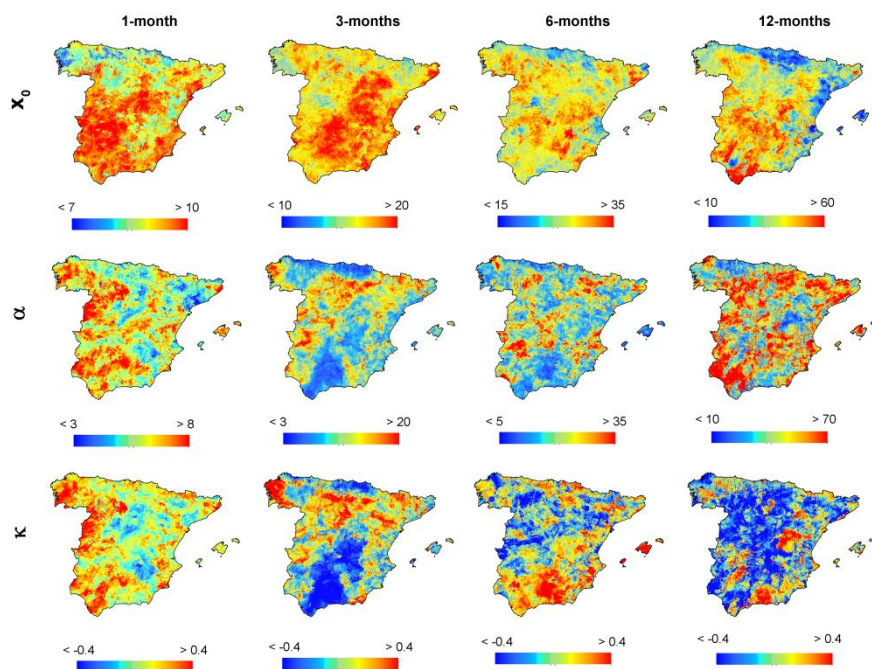
**Figure 8: Spatial distribution of the parameters of the GP distribution for the SPEI duration series.**

5
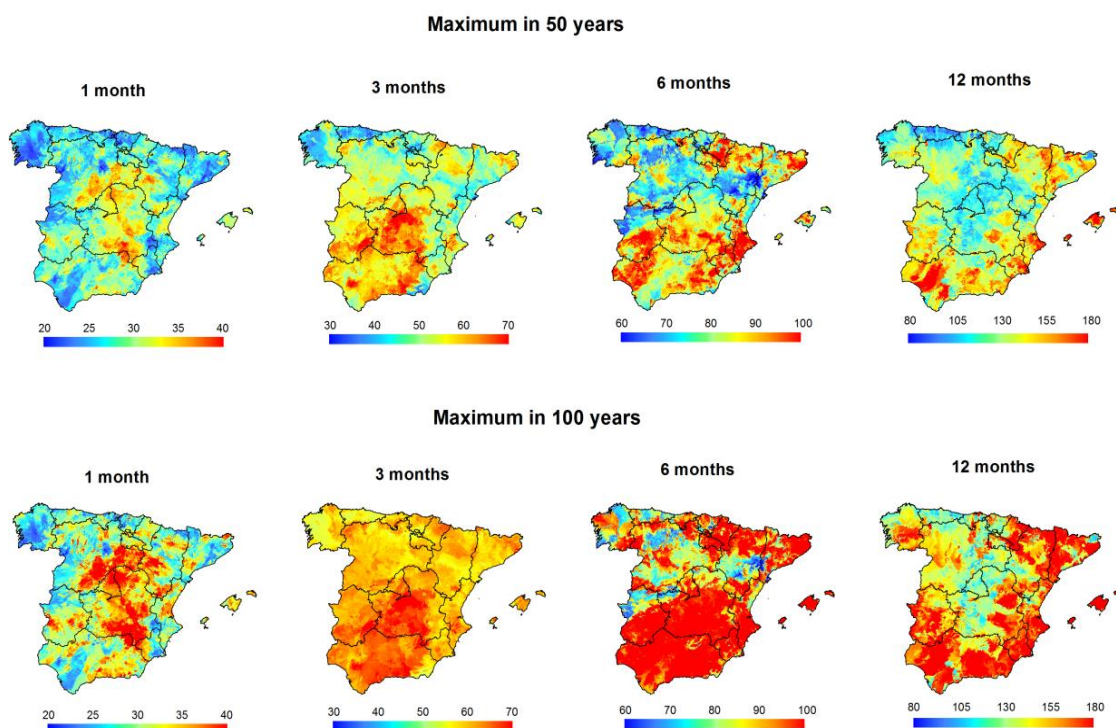
**Figure 9: Spatial distribution of the maximum drought duration (in weeks) from the 1-, 3-, 6- and 12-month SPEI series in a period of 50 and 100 years.**

5
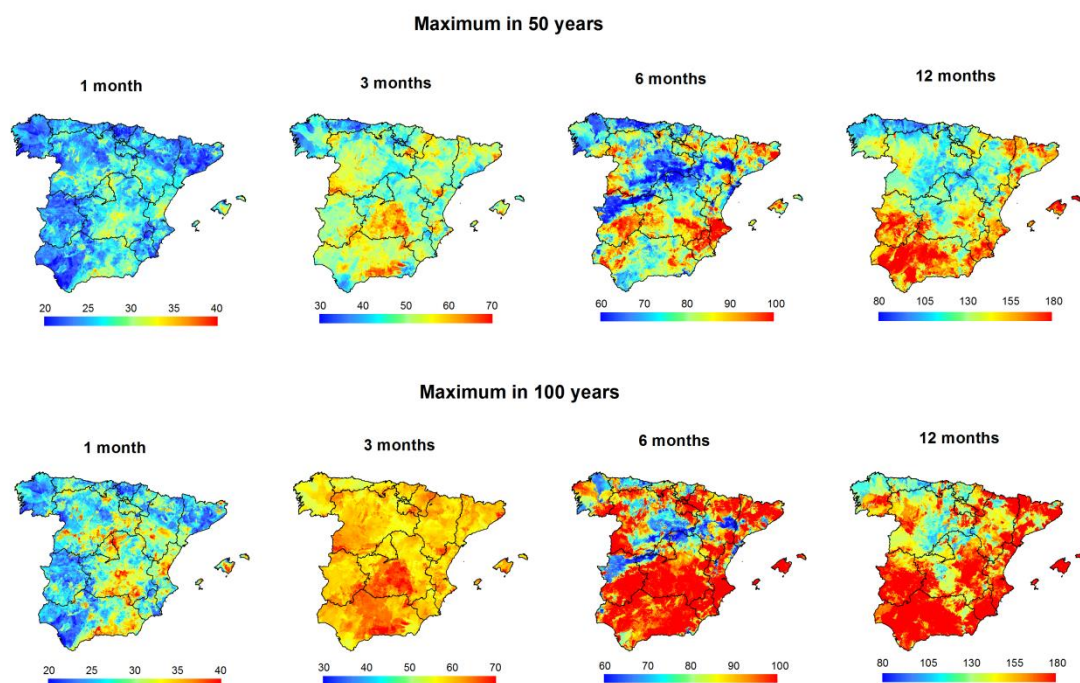
**Figure 10: Spatial distribution of the maximum drought duration (in weeks) from the 1-, 3-, 6- and 12-month SPI series in a period of 50 and 100 years.**
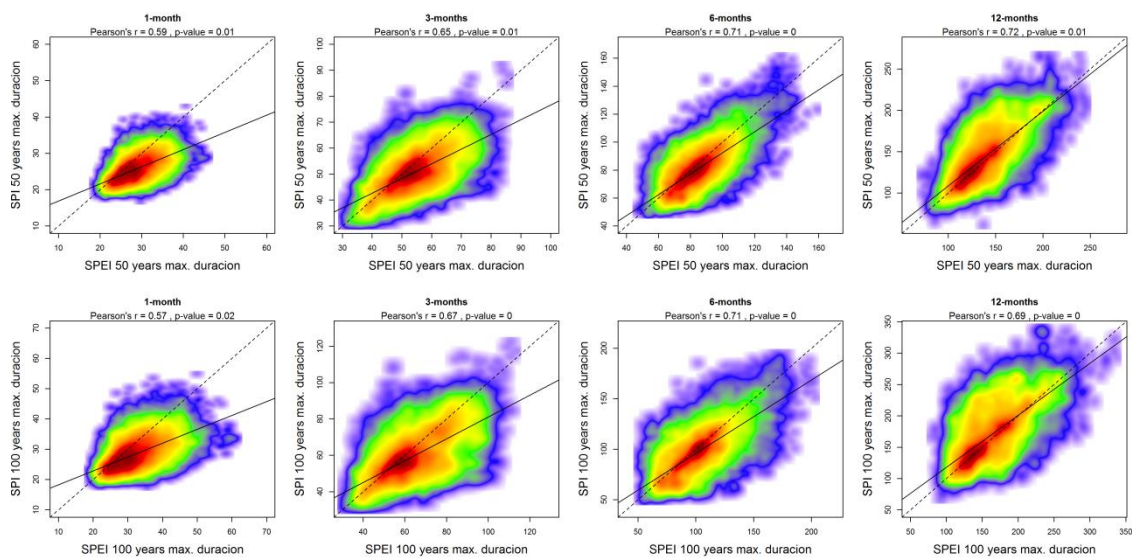
5

**Figure 11:** Scatterplots showing the relationship between the maximum drought duration (in weeks) expected in a period of 50 and 100 years considering 1-, 3-, 6- and 12- SPEI and the SPI. Colors represent the density of points, with red denoting the highest density. Given the large sample used, the significance of the Pearson's r coefficients was estimated by means of a Montecarlo approach using $10^3$ random samples, with each sample containing 30 cases.